CORONA AND RADIO INTERFERENCE ON POWER LINES

by

RABIE ABDEL FADEEL MOSTAFA

B. S., Assiut University, U.A.R., 1963

A MASTER'S REPORT

submitted in partial fulfillment of the

requirements for the degree

MASTER OF SCEINCE

Department of Electrical Engineering

KANSAS STATE UNIVERSITY
Manhattan, Kansas

1968

Approved by:

gary johnson
Major Professor

TABLE OF CONTENTS

LIST OF TABLES

LIST OF FIGURES

CHAPTER I

INTRODUCTION AND MECHANISM OF CORONA

Introduction

High-voltage power lines are subject to a type of energy loss that does not occur on lines operating at low voltage. The high electric field strength in the region immediately around the high-voltage conductors causes ionization of air in that region. Electrons are accelerated by the force of the electric field and if the voltage is sufficiently high, electrons will gain enough energy to enable them to ionize air molecules by collision. If the electric field strength exceeds a critical value, ionization becomes cumulative, and appreciable loss of power from the high-voltage line results. The luminosity that accompanies profuse ionization is called corona; it is readily visible at night about the surface of overstressed high-voltage conductors. Under ideal conditions, it appears as a uniform glow, but more commonly it is in the form of a multitude of brush discharges from minor roughness and irregularities of the conductor surfaces.

At each of the many discharges a pulsating stream of electrons enters or leaves the conductor according to its instantaneous polarity. All these fluctuating emissions cause oscillations of random phases over a continuum of frequencies up to several hundred megacycles. The electric and magnetic fields associated with the oscillations may interfere with radio communication equipment near the power line.

The objectives of this report are:

1. To present data from single phase, single conductor laboratory tests which were made in the electrical engineering department, Assiut University, U.A.R.
2. To study the analyzed portion of the results on the fair-and-foul-weather line losses and radio noise.
3. To present data for insulator losses and for losses caused by corona on the line conductor.
4. To show the effects of load currents on corona losses in fair and foul weather.
5. To correlate the radio noise data from the test line, which is affected by radio frequency standing waves, with long line performance.
6. To show the effect of weather on radio noise for the conductor arrangements and explain the large variations which characterize it.
7. To provide a basis for predicting corona losses and radio noise with a useful degree of accuracy in advance of line construction.

Mechanism of Corona and Definition of Terms Related To It

(A) Mechanism of Corona:

The ionization processes starts during the negative half-cycle with the free electrons found in the atmosphere (Pearson, 1961). As the potential gradient is increased, these free electrons gain enough energy to ionize neutral atoms and cause

electron avalanches in the high-gradient regions. Due to the electric field, the ionized atoms or positive ions are attracted towards the conductor, whereas the electrons having a negative charge move away from the conductor. In addition to the radial motion of charges, there also will be a small axial motion resulting from charge concentrations. Since the mobilities of positive ions and negative electrons are quite different, the electrons can move for some distance, whereas the positive ions remain relatively immoble during a half-cycle. When distant from the conductor, the electrons can attach themselves to oxygen atoms if the electric field becomes weak or the instantaneous value of the applied voltage approaches zero. This attachment, however, is quite weak and the electrons can be set free again by an increased gradient. The attachment also can take place in the high-gradient regions between successive collisions when the electron energies become small.

At the end of the negative half-cycle, there will be a negative space charge, distant from the conductor, and a positive space charge near the conductor surface. When the negative corona is confined to a single point on the conductor, the negative space charge can be visualized as a cone whose tip is directed toward the conductor. The shape of the positive space charge in this case is similar to that of the negative space charge, except that its height will be much lower and the base of the cone will be on the conductor.

Of course, concentrations of charges in these two clouds of space charges will also be different. When the conductor

is made positive, the positive space charge will slowly move away from the conductor, whereas the negative space charge will move towards the conductor at much higher speed. As the cloud of negative space charge approaches the conductor, the gradient in the intervening space is increased to a point where a spark discharge takes place. When this occurs, the two space charges are neutralized and the process can start again in the next negative half-cycle. The occurrence of the spark discharge tends to explain the single-impulse characteristics and the general appearance of the positive corona. It also explains the unstable nature of the positive corona. Since this corona depends largely on the amount and the concentration of negative space charge, it seems reasonable that it would take several negative half-cycles to produce proper conditions for the spark discharge.

If the d-c voltage were applied, the transient effects are the same as for a-c, but after steady state is reached no further discharge would occur until the charge leaks off through the air dielectric and the voltage across the gas space is again restored to that required for breakdown (AIEE Working Group on Definitions, 1963). Since such leakage is usually slow, comparatively few corona pulses will occur. If, however, the applied voltage is a-c and is of sufficient magnitude, it may continue to rise until the gradient across the gas is again sufficiently high for breakdown and another pulse will occur. Such pulses wil occur to the peak of the applied voltage wave when the voltage begins to drop. On the next half-cycle reverse discharges will

occur since the field caused by the applied voltage is augmented by that caused by the charge deposited on the previous half-cycle. Such discharges, occurring regularly on each half-cycle, are termed continuous corona. Although the applied a-c voltage is somewhat below that required to initiate corona, a surge may cause a corona pulse to occur. On the next half-cycle the voltage near the conductor may again exceed the corona onset value, owing to augmenting of the field by the deposited charge. Such discharges will cease after several half-cycles and are known as intermittent corona.

(B) Definition of terms related to corona:

The terms to be defined have been divided into two categories: (1) those dealing with phenomena and (2) those concerned with measured quantities. These definitions have been presented by the AIEE Working Group on Definitions (1963).

Phenomena

1. Ionization: The process by which neutral molecules or atoms dissociate to form positively and negatively charged particles. Those species which are positively charged are positive ions, while those negatively charged may be negative ions or electrons.
2. Electrical discharge: The phenomenon accompanying any ionization in a dielectric which occurs as a result of the application of an electric field. Two classes of discharge may be distinguished:

(a) Those discharges which, once initiated, do not require for their continuance a source of externally supplied electrons or ions are termed self-sustained discharges, and usually require the minimum critical voltage for their inception and extinction.

(b) Those discharges which do require for their continuance a source of externally supplied electrons or ions are termed non-self sustained discharges and do not possess fixed minimum critical voltages for their inception or extinction.

3. Corona: Self-sustained electrical discharges in which the field-intensified ionization is localized over only a portion of the distance between the electrodes. This may occur either because of the field nonuniformities such as are present at electrode edges, points, or wires, or over non-uniformly conducting surfaces, or because the voltage across one of two or more dielectrics in series between the electrodes does not attain the minimum critical value required to support self-sustained discharges in this dielectric.

4. Corona pulse: A corona discharge which builds up and extinguishes itself in a short period of time (usually a fraction of a microsecond). This often-encountered property of corona is a result of the accumulation of charges produced by the discharge with a consequent reduction in voltage in the discharging region to below the critical value required for extinction. As the applied voltage rises or as the

accumulated charge flows from the system, further corona pulses occur.

5. Continuous corona: Corona pulses which recur at regular intervals for periods of several minutes or more.
6. Intermitted corona: Corona pulses which recur at regular intervals for periods of from several cycles of applied voltage to seconds with similar or longer periods between discharges.
7. Corona Streamer: A highly localized filamentary type of corona discharge.

Measurements

1. Corona detector: A device for the detection of corona in a specimen. The sensitivity of the detector must be specified for significant results.
2. Corona inception voltage: The minimum voltage which must be applied to the system to initiate continuous corona.
3. Corona extinction voltage: The maximum voltage applied to the system at which continuous corona, once initiated, ceases.
4. Apparent corona pulse charge: The quantity of charge supplied to the system terminals from the voltage supply after a corona pulse has occurred. It is related but not equal to the quantity of charge actually flowing in the localized discharge.
5. Apparent corona current: The sum of the apparent corona pulse charges divided by the time of sampling.

6. Corona loss: The power dissipated in the system owing to corona discharges. In measuring this quantity care must be taken to insure that dielectric losses are negligible or can be allowed for.

CHAPTER II

EFFECT OF CONDUCTOR DIAMETER AND PHASE SPACING ON FLASHOVER AND VISUAL CORONA VOLTAGES

When the potential difference between the conductors of an overhead transmission system exceeds a certain definite value (the visual critical voltage of the line) a hissing sound is heard, and the conductors are found to be surrounded by a luminous envelope to which the name corona has been applied (Waddicor, 1928). The luminous envelope is composed of air which has broken down and become temporarily conducting under the high electrostatic stress, and its effect is equivalent to increasing the diameter of the conductors. The breakdown starts first near the surface of the conductor, as the electrostatic stress or potential gradient has its maximum value there, and the thickness of the conducting layer of air increases with an increase of potential difference. If the conductors are very close together the formation of corona involves an increase in the potential gradient between them; the corona spreads farther, the process continues until flashover occurs. In this case immediate disruption takes place, and no stable corona can be formed.

Laboratory tests were made in the Department of Electrical Engineering, Assuit University (Mostafa, 1964) to show the effect of phase spacing and diameter of the conductors used in single phase, parallel transmission lines.

The experimental apparatus used in those tests were:

1. High-voltage transformer 380/150,000 volts.

2. Regulating transformer 220/0-400 volts.
3. Some pairs of parallel cylindrical smooth copper wires with different diameters, with lengths 1.5 meters.
4. Water resistance.
5. Two sphere gap to measure the high voltage. The chart of the sphere gap which indicates the relation between flash-over voltage and distance between the two spheres was availble.
6. Oscilloscope to show the wave form of corona current.
7. Remote control disc.

The connection diagram of the test is shown in Figure 1. The test was carried out in a darkroom and the temperature and barometric pressure were 28°C and 76 cm., respectively.

The results of this test, which are shown in Figure 2 indicate that the flashover voltage V_{fo} across the gap between two parallel conductors is dependent upon the phase spacing, and that a distance less than 30 times the radius of the conductor the flashover occurs at a voltage less than the visual critical voltage V_v. At that distance the critical voltage V_c is directly proportional to the radius of the conductor, which at a diameter of 3.5 mm. is equal to about 26 KV (r.m.s. kilovolts). The part of the curve of the visual critical voltage at distances less than 30 times the radius of the conductor is obtained by extending the curve for distances larger than this value.

The potential gradient at which complete disruption of a dielectric occurs is called the disruptive strength or dielectric

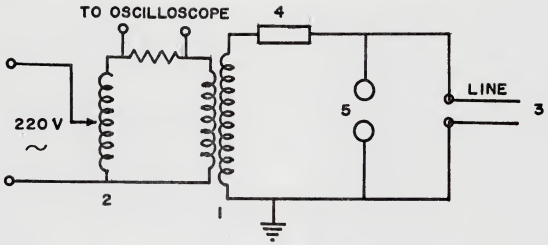

Fig. 1. Connection Diagram for Flashover and Visual Corona Test.

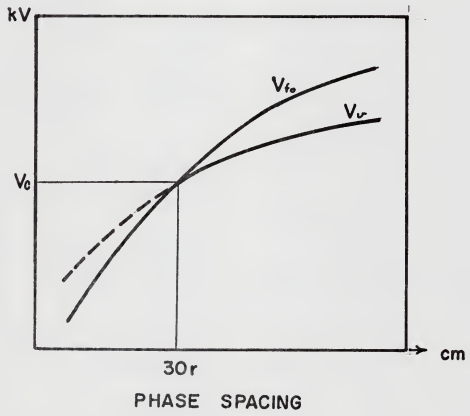

Fig. 2. Flashover and visual critical voltage vs. phase spacing.

strength of the material (Waddicor, 1928). For air at a barometric pressure of 76 cm., and a temperature of 25°C, it is E_o=30, KV (peak value) per cm. The dielectric strength of air is proportional to its density over a very wide range, and thus directly proportional to the barometric pressure, and inversely proportional to the absolute temperature. Taking the density of air under the above standard pressure and temperature conditions as being equal to unity, the relative density at a pressure of b cm., and temperature of t°C, is

$$\delta = \frac{3.92b}{273+t} \qquad (1)$$

and the dielectric strength under these conditions is $E_o\delta$.

In a uniform dielectric field such as exists between parallel plates the potential gradient has a constant value at all points. If the voltage is gradually increased, as soon as the breakdown gradient of 30 KV/cm. is attained (assuming standard pressure and temperature conditions); the air breaks down and flashover occurs, short-circuiting the plates.

If the dielectric field is not uniform, for instance, the field between two parallel wires or two spheres, then with increasing voltage the breakdown gradient will not be reached simultaneously throughout the entire field, but is first attained at the surface of the wires or spheres.

In the case of parallel wires it has been shown (Waddicor, 1928) that the potential gradient at the surface of the conductors is given by

$$E_m = \frac{V}{r \log \frac{d}{r}} \quad \frac{KV}{cm} \tag{2}$$

where V is the potential to neutral, both E_m and V being expressed in r.m.s. values. When the disruptive gradient of air is reached at the conductor surface, equation 2 becomes

$$E_o = \frac{V_o}{r \log \frac{d}{r}} \tag{3}$$

or

$$V_o = E_o r \log \frac{d}{r}$$

V_o is known as the disruptive critical voltage. In practice, corrections have to be applied to this formula for air density and surface conditions of the conductor, the complete formula being

$$V_o = 21.1\, m_o\, r\, \delta \log \frac{d}{r} \text{ KV to neutral (r.m.s.)} \tag{5}$$

where r = radius of conductor in cm.

d = spacing between centers of conductors in cm.

m_o = 1 for polished wires

= 0.98 - 0.93 for roughened or weathered wires

= 0.78 - 0.80 for stranded conductors.

In the case of parallel wires it is found that visual corona does not begin at the voltage V_o at which the disruptive gradient of air E_o is reached, but at a higher voltage V_v called the visual critical voltage.

Peek (1911) has shown that the relation between the visual critical voltage gradient of air and the radius of the conductor can be expressed by the formula

$$E_v = E_o \delta \left(1 + \frac{0.3}{\sqrt{\delta r}}\right) \tag{6}$$

The complete formula for visual critical voltage is, from equations 2, 5, and 6,

$$V_v = 21.1\, m_v \delta r \left(1 + \frac{0.3}{\sqrt{\delta r}}\right) \log \frac{d}{r} \text{ KV to neutral (r.m.s.)} \tag{7}$$

$m_v = m_o$ for wires (1 - 0.93)

= 0.72 for local corona on stranded conductors

= 0.82 for pronounced corona on stranded conductors

CHAPTER III

CORONA LOSS IN FAIR AND FOUL WEATHER

Initially, losses of energy were of primary interest and, as early as 1912, F. W. Peek, Jr., stated that the effect of snow was greater than that of any other weather condition. Tests on actual lines sometimes confirmed Peek's statement; sometimes not. Many attempts were made to find some quantitative relations between atmospheric conditions and corona losses.

Fair-Weather Corona Loss

Fair-weather corona loss at normal operating gradients is insignificant in comparison with foul-weather losses. For this reason, no concerted effort was made to determine all meteorological influences on this loss, and only a few general observations will be reported.

Project EHV (extra high-voltage) tests on a-c lines have demonstrated (Anderson, et. al., 1966) that humidity and relative air density have only a minor influence on fair-weather transmission line corona loss. For example, Figures 3 and 4 show how the median fair-weather corona loss for a three 1.465 inch diameter plover configuration at 45.5 foot phase spacing at 700 KV was observed to vary with humidity and relative air density respectively. These figures are obtained from histograms of corona loss vs. relative humidity and air density by plotting the loss median against the average of each class of the other

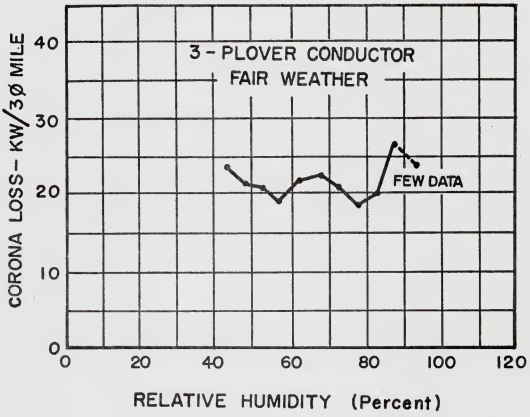

Fig. 3. Corona loss at 700 KV vs. relative humidity.

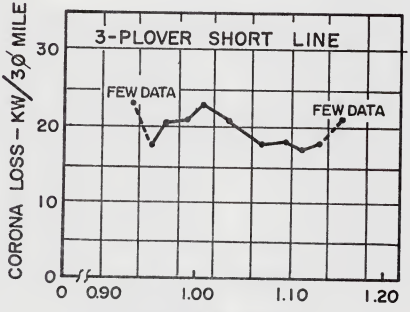

Fig. 4. Median fair weather corona loss at 700 KV vs. relative air density. Conductor diameter = 1.465 inches. Phase spacing = 45.5 feet.

variable. Obviously, as the condition of 100 percent humidity is approached, the formation of discrete water droplets on the conductor surfaces and water films on the insulator surfaces will cause the losses to rise appreciably. For the usual fair weather conditions the only pronounced variation in corona loss is caused by variations in particle concentrations on the conductor surface. These particles are usually dust particles, minute fragments of vegetation and insects.

Losses During Overvoltage Conditions

Although fair-weather corona losses are not economically significant at normal operating voltages, they become of great interest during periods of sustained overvoltages created by EHV system disturbances (Anderson, et. al., 1966). Corona loss, since it represents an additional impedance between conductors and ground, acts in the direction to suppress severe overvoltages that might otherwise appear. This subject is still undergoing study. However, some of the observed characteristics of both transient and steady-state corona observed on Project EHV test lines are of interest in such a study, and will be reported here rather briefly for both fair-and-foul weather conditions.

The significant parameters influencing fair-weather corona loss are voltage, conduction configuration, and surface gradient. The increase in fair-weather corona loss with voltage for a test line is shown in Figure (5). Up to approximately 500 KV, already a moderately severe overvoltage condition, the only corona of

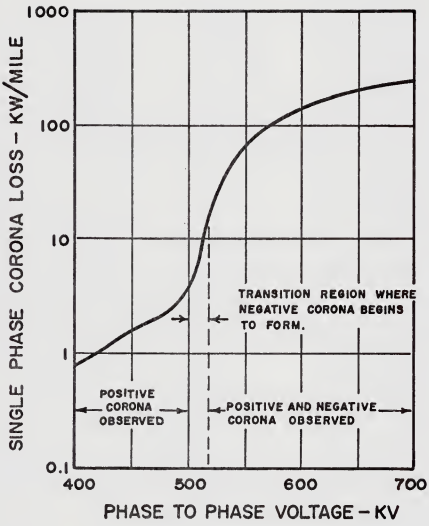

Fig. 5. Typical fair-weather corona loss. In a single 1.465-inch diameter Plover ACSR conductor showing transition stages of corona loss. Line length = 2900 feet. Phase spacing = 38.5 feet. Operating design voltage = 300 KV. (Anderson, et. al., 1966).

any appreciable magnitude noted on the test line was of positive polarity. Corona losses in this region increased with approximately the sixth power of the voltage. A transition region appears at about 500 KV where negative corona also begins to be apparent and above 520 KV significant amounts of both appear. Figure 5 indicates an abrupt increase in corona loss at this transition region as a result of the additional contribution of the negative corona. Also from Figure 5, a 300 KV line 100 miles long would have a total loss of about 36 MW at twice normal voltage. This is approximately 16% of the surge impedance loading.

Figure 6 shows sample sets of switching-surge voltages applied to the single-conductor EHV line, and the corresponding corona currents. In this particular illustration the voltages were produced by an impulse generator, although circuit-breaker generated surges were also studied and gave similar results. The test line was a single plover 300 KV line having an assigned nominal line-to-ground voltage of 245 KV crest. Switching surges of 1.88 and 2.86 times normal are shown. For these surges, emission of significant positive polarity corona current began at about 400 KV or 1.6 times normal crest for both waves. This is approximately the level at which a major increase in 60 cycle corona effects appear (see Figure 5). The current built up to its peak value in less than 100 microseconds for both surges, and then decayed slowly to a low and relatively constant value. As a first approximation, it appears that the corona envelope forms very rapidly for switching surges; and once formed, requires

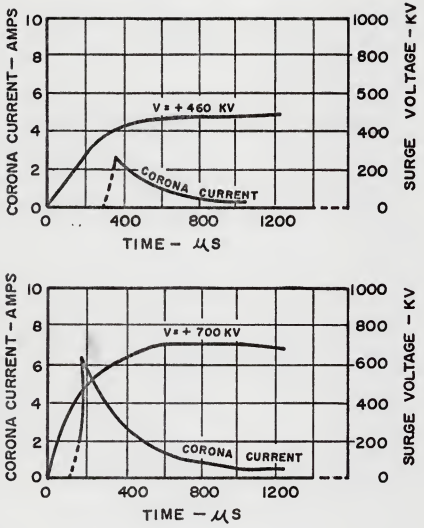

Fig. 6. Simultaneous switching-surge voltages and corona currents on a 300-KV single-Plover transmission line 2900 feet long.

only enough current to modify the envelope to adjust for any further voltages changes. Therefore, once it has formed, the current is roughly proportional to the derivative of the voltage; that is, its nature is capacitive except that it does not return as much energy as the voltage falls. It is obvious, however, that for a flattopped wave, the corona current will not decrease to zero, as it would for a pure capacitance when a constant crest voltage is reached, but instead approaches the normal steady-state d-c corona. It is generally apparent that short-duration surges will undergo the greatest distortion by corona loading and that waves with slow fronts and flattops will be affected the least.

Foul-Weather Corona Losses and the Effect of Load Currents

Foul-weather corona loss for 500 and 700 KV transmission lines may reach a value of 500 KW/mile or more at operating voltages, and can create both an appreciable energy loss and a significant influence on reserve requirements (Anderson, et. al., 1966). Because of their possible economic significance, these losses are worthy of extensive study. It was found that foul-weather losses are extremely sensitive to small amounts of precipitation. Unfortunately, these are in the precipitation range where rates are very difficult to measure with any precision using standard weighing-bucket measuring devices. Rain rates from 0 to 0.02 in/h were determinable only by estimate, those above 0.02 in/h were of working accuracy. In the case of snow,

the precipitation rate was established only by visual observation as trace, light, medium, or heavy, rather than as an arithmetical rate.

Conductor-heating effects caused by load currents of 550 amperes reduced corona losses during dew, fog or frost to values of low economic significance. During rain conductor-heating currents did not significantly modify corona-loss values. For periods of snowfall, heating currents generally decrease corona losses. The reduction caused by the action of the melting and sticking of snowflakes, did not reduce the maximum values observed.

Table I (Taylor, et. al, 1965) below gives typical values of corona loss measured during various weather conditions and, in the case of rain, correlates the rate of rainfall against the level of corona loss observed in the period.

Table I: Typical Foul-Weather Corona Loss, Kilowatts per Mile, 2 by 1.602 by 18 Inches, 525-KV Line Voltage, 35 Foot Phase Spacing

	Outside Phase		Center Phase		3-Phase Total	
	Ave.	Highest	Ave.	highest	Ave.	Highest
Light short rain, 0.001 to 0.015 in/min.	25	47	45	55	95	149
Intermittent medium rain, 0.004 to 0.010 in/min., average of 0.006 in/min.	40	45	67	70	147	160
Long heavy rain, 0.01 to 0.06 in/min. average 0.021 in/min.	40	60	67	90	147	210
Fog	25-35		30-55		80-144	
Heavy wet snow	50		55		155	

Insulator Loss and Separation of Losses

The losses measured on transmission lines consist almost entirely of corona losses and insulator losses (LaForest, et. al., 1963).

Insulator losses in watts per string are plotted against the square of per unit equivalent line-to-line voltage indicates that fair-weather leakage resistance is independent of voltage as shown in Figure 7.

In Figure 7 the losses below the per-unit voltage square value of 1.2 fall on a straight line, almost passing through the zero point. For values above the per-unit voltage square of 1.2, the losses increase very rapidly. The break-off point represents a general onset of corona on the conductors. The losses shown above the straight line are conductor corona losses; the straight line represents losses proportional to the square of line voltage similar to insulator losses. Other losses may also be included in this apparent insulator loss. There are losses caused by eddy currents in towers induced by the 3-phase field, I^2R losses from charging currents, and ground losses from zero sequence currents. These contributions may be small individually, but in total may account for a portion of the apparent insulator losses which in this case cannot be explained from the single-phase insulator loss measurements. There is another possibility. The apparent insulator loss of 3,100 watts at one per-unit voltage in Figure 7 approximately corresponds to 80 watts per string. Since this loss was derived from 3-phase tests, it is possible the

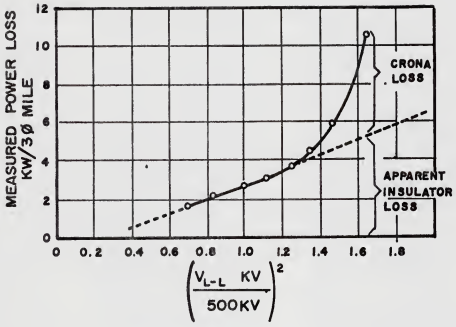

Fig. 7. Line loss as a function of per unit line-to-line voltage squared. Two ACSR 1.465 inch-diameter cables per phase, bundle spacing 18 inches, phase spacing 385 feet, length of the line 4.3 miles, and line voltage 525 KV.

voltage distribution is poorer and the losses are higher than that for single phase tests.

Insulator losses are nearly the same for rain and humid conditions, at least for vertical insulator strings with grooves on the underside to break up the wetted surfaces. For driving rain, or rain on horizontal strings, the insulator losses would be higher. Insulator losses have a strong dependence on relative humidity. The 80 watts per string of the previous example is probably for high relative humidity conditions. The losses may be only a few watts per string for a relative humidity below 50%. Above 50% the losses increase almost exponentially. This increase is believed to be caused by the buildup of leakage current in a surface film which increases at high humidity rather than being caused by condensation on the porcelain.

Shielding rings help to reduce this leakage current and also help to prevent corona. These are placed at the line end of the insulator strings.

A Corona-Loss Equation

The formula for loss of power in fair weather derived from experimental data by Peek (1911) is

$$P_c = \frac{390}{\delta}(f+25)\sqrt{\frac{r}{d}}\,(V-V_o)^2\ 10^{-5}\ \text{KW/mile/phase} \qquad (8)$$

where V = r.m.s. KV to neutral

f = frequency in cps

The other constants have their former values.

The approximate loss under storm conditions is obtained by taking V_o as 0.8 times its fair-weather value. As a matter of fact, with perfectly smooth and cylindrical conductors no loss occurs until the visual critical voltage is reached, when the loss suddenly takes a definite value equal to that calculated by the quadratic law with V_v as the applied voltage. It then follows the quadratic law for all higher voltages. With the roughened and weathered conductors used in practice, however, the quadratic law is approximately followed over the whole range of voltage starting at V_o.

The other corona loss equation for single and bundled conductors was developed by Nigol and Casson (1961). The basic form of the equation is

$$P_c = Kfr^2 \frac{\Delta\rho}{2\pi} E_e^2 \ln \frac{E_e}{E_o} \qquad (9)$$

where

P_c = corona loss per conductor, KW/mile

K = conditional constant for given weather and conductor surface conditions

f = frequency in cps

r = radius of conductor, cm

E_e = effective surface voltage gradient, KV(rms)/cm

E_o = critical surface voltage gradient for given weather and conductor surface conditions, KV(rms)/cm

$\Delta\rho$ = angular portion of conductor surface in corona, radians.

For single conductors at normal phase spacing the gradient E_e is essentially constant over the conductor surface and it is

CHAPTER IV

RADIO INTERFERENCE GENERATION, PROPAGATION, AND ATTENUATION

(a) Generation

Radio interference (RI) is produced by corona, sparks, and similar effects associated with a high voltage transmission system. These phenomena are characterized by pulsating charges and currents. From Faraday's law the fields produced by these currents are proportional to $\frac{dB}{dt}$ and to $\frac{di}{dt}$. Aside from $\frac{di}{dt}$ the circuit conditions linking the flux between conductors through the geometry of the circuit determine how great the influence will be (Loeb, 1965). Impulsive discharges such as the Trichel pulse corona and the heavy breakdown streamers have $\frac{di}{dt}$ on the order of 10^6 to 10^7 amp/sec. Small sparks where instantaneous currents in the hundreds of amperes arise in 10^{-6} seconds can lead to still higher values. These induce surges of currents in any conductor cut by the flux. They lead to damped electrical oscillations in the conductor lasting for some time after the triggering source has ceased. Such oscillations are transmitted for some distance along the line and are also radiated into space. The current pulses, being of complicated form, give rise to many harmonics covering the usual broadcast band and invading the higher frequencies.

The sources of such RI are essentially three: (1) Electrical breakdown of insulators inside the generating and distributing complex. These involve corona and sparks in the insulating oils of circuit breakers, switches, and transformers.

(2) Breakdown over the surfaces of insulator strings and at regions of high electrical stress where supports of various types are embedded in concrete. (3) Corona discharges from the conductors themselves. The type 1 interference does not concern us. The second type at the insulators has been extensively studied and improvements in design that are not too costly have, or should be able to, reduce this source to a minor one. It is true that insulator strings have the insulator surfaces coated with dusts, sea salts from fog, fume condensates from industrial contamination ranging from sulfuric acid and hygroscopic sulfates to carbon and oily deposits. The dusts will be coated with salts and hygroscopic materials so that they become conducting. They are most troublesome when the humidity is such as to give a conducting coating, leaving small dry isolated patches over which small sparks can occur. On the other hand, the discharges from metal embedded in concrete are less serious when the humidity is high, since these surfaces become sufficiently conducting so that sparks and discharges from small sharp points no longer occur, as these are smoothed over and gaps are bridged.

The real concern is the corona from the long high-tension conductors. Laboratory investigations of corona discharges show that they may exist in three different stages which, for convenience, are called glow, brush, and plume discharges (Newell, Warburton, 1956). Glow discharges, which generally are caused by tiny defects on the conductor surface, occur at or near the critical visual corona voltage, produce no audible corona, and usually generate a radio influence voltage (RIV) level

of less than 100 μv as measured by the standard National Electric Manufacturers Associaton (NEMA) circuit. Brush discharges, so named because they resemble the bristles of a brush, occur on the conductor surface at voltages above the visual corona voltage. They produce audible corona and, depending upon the 60-cycle voltage, an RIV level ranging from 100 to about 5,000 μv when measured on 25-foot sections of conductors. Plume discharges have a trunk-like spark extending 2 or 3 inches from the surface and a luminous head which may be 8 or 10 inches long and several inches in diameter. They appear suddenly on a conductor as the voltage is raised and they produce considerable audible noise and an RIV level which starts at about 10,000 μv and which may go as high as 100,000 μv on a 25-foot conductor specimen. They are usually initiated by a fair-sized surface defect such as a nick on a strand, a displaced strand, or some foreign material on the conductor surface.

(B) Propagation

The conductor noise level measured directly at any point of a noisy line and the resulting noise field RI are cumulative effects, within a limited bandwidth, of a large number of noise signals generated at various distances and times. Original amplitude or location of noise sources cannot be identified by any known physical method. In dealing with such random but repetitive quantities, some assumptions must be made, then, and special methods of analytical interpretation are applied.

Consider a single signal at a fixed frequency traveling along a system of parallel conductors at a constant height

above a conducting ground. This may represent a hypothetical frequency component of a single noise impulse injected into a conductor. For the case of a single frequency signal propagation, J. R. Carson and R. S. Hoyt (1927) formulated a solution by applying "the generalized telegraph equation" to a multi-wire system. The solution indicated the existence of "natural modes" of propagation, derived from the roots of the characteristic determinant of the set of equations. In 1941, S. O. Rice, applying matrix algebra, developed a solution of transmission line equations as an extension of the work of Carson and Hoyt. A relatively simple method of analyzing power-line carries (PLC) propagation on a 3-phase line by means of symmetrical components was published by A. Chavallier (1945).

Modern analysis of corona pulse propagation may be attributed to Adams (1956b). His method is basically similar to that of Pipes (1937) but he demonstrated the effects of power line parameters on the natural mode components or eigenvectors, calculated from the conductor system matrix. Furthermore, Adams directly applied natural modes to the electromagnetic field at ground level; that is, to the transverse field RI profile. Various recent theoretical and experimental investigations (Perz, 1963) refer to Adams' work (1958) on many aspects of corona noise generation, propagation, and the field strength of RI, and present analytical methods readily handled by digital computers.

Certain characteristics of electromagnetic wave propagation along a system of parallel conductors above a conducting ground simplify the analytical solution of corona noise propagation on

power lines (Perz, 1963). Waves are in the form of equi-phase planes, perpendicular to the conductors and ground. The electric field is perpendicular to the magnetic field, and at ground level is partially vertical. Since the spacings between the conductors and the height of the line above ground are all small as compared with the wavelength of RI frequency components, even at broadcast frequencies, the radiation losses can be neglected. Thus, analysis of the RI field simplifies to the elementary calculation of field intensities around conductors carrying d-c charges.

Furthermore, at any point of the line the conductor noise voltages and currents are linearly related to form a set of "n" linear equations with real coefficients, where n is equal to the number of conductors. The coefficients which represent the self and mutual impedances are real because, at this stage of analysis, the line is assumed to be lossless and the ground perfectly conducting. In calculating impedances the conductors are assumed to be perfectly parallel to ground and to each other; the height of the conductor is usually considered to be equal to the midspan height, plus a third of the sag.

In evaluating the cumulative effect of distributed corona noise sources on a long line, different attenuation coefficients are attributed to the natural mode components. The coefficients can be evaluated from tests made on long lines energized by a system of generators producing voltages and currents characteristic to each single mode. The empirical values of mode attenuation are in good agreement with those calculated by a method developed

by Adams and Barthold (1960), who estimate the effect of the proximity of lossy ground on the attenuation.

The importance of the lossy ground effect on the propagation of electromagnetic waves had been already recognized by the earliest investigators (Zenneck, 1907). The natural modes of propagation, which depend on the geometry of the system of parallel conductors, are intrinsically orthogonal so that no mutual coupling exists between modes. It is generally accepted that the orthogonality of mode currents or voltages is maintained during propagation along sagging conductors above a lossy ground.

This outline of developments in learning to analyze the propagation of electromagnetic waves along a system of parallel conductors gives some insight into the fundamentals and limitations of recent methods of calculating corona noise on long lines. The results of noise analysis as applied to power lines with skywires have been presented, for example, by A. R. Abboushi and L. O. Barthold (1961). The main steps of such an analysis are:

1. Calculation of the constants of a line considered as a system of parallel conductors.

2. Evaluation of noise current per unit length of each conductor at a specified frequency and bandwidth, based either on calculation of gradients and the resulting generation, or an actual noise measurement of short samples of the conductor.

3. Resolution of generated noise currents or voltages on each conductor into natural mode components, derived from the impedance matrix of the line constants of point 1.

4. Calculation of natural mode noise currents on a long line by assuming a uniform distribution of uncorrelated noise sources. The mode components of a single source are completely correlated at the point of generation but, in calculating the resultant mode currents at a distance, the modes are considered either completely correlated or completely uncorrelated. Specific mode attenuation coefficients are attributed to each mode, and it is assumed that the mode orthogonally is not affected during propagation.

5. Calculation of RI field profiles, corresponding to the currents of each mode, and the resulting RI field at a specified lateral distance from the line.

6. Calculation of profiles of a short test line, following a procedure similar to that in point 5.

This method leads to a resulting noise current and RI field intensity expressed in r.m.s. values, even for correlated modes of elementary currents. Therefore, the accuracy of the calculated values could be confirmed by measurements with an r.m.s. noise meter. One limitation of this method is that the attenuation constant must be known.

(C) Signal-to-Noise Ratio (Attenuation)

Radio interference from power systems has been a public relations problem for over thirty years (Mather, Gehrig, 1961). The operating companies have assumed the obligation to construct their lines and equipment in such a manner as to inflict the least practicable nuisance on the general public. Unfortunately, no national standards have evolved over the years as a guide to the

adequacy of utility practice in this respect. The absolute values of interference in themselves are not wholly significant--conditions in one locality may be entirely satisfactory and the same conditions at another point in the system may be intolerable. This arises from the fact that interference must be considered in relation to the radio station signal strength. Listening tests have established that the listener is not aware of the background noise if the voltage level of the interference is less than one-fortieth of the radio station signal strength at a given receiver. In urban areas, adjacent to the radio transmitters, power line interference can easily be held to values less than one-fortieth of the radio station signal strength. In rural areas, however, the listener may be fifty miles or more from the transmitter and the forty-to-one ratio is not as easily achieved. Consequently, in these areas, a signal-to-noise ratio of twenty-five-to-one has been selected as a reasonable objective. At this level, background noise is audible but not objectionable to most listeners.

Normally, the radio signal in a particular neighborhood is quite uniform for all listeners. The radiated interference (RI) from a transmission line, however, drops off very rapidly with distance from the line, as shown in Figure 8. Consequently, the distance from the line determines the signal-to-noise ratio for a given receiver. In the example illustrated, if a listener living 200 feet from the transmission line prefers to listen to radio station "B", he will not be affected by the transmission line (except possibly during heavy rain-fall), whereas a listener

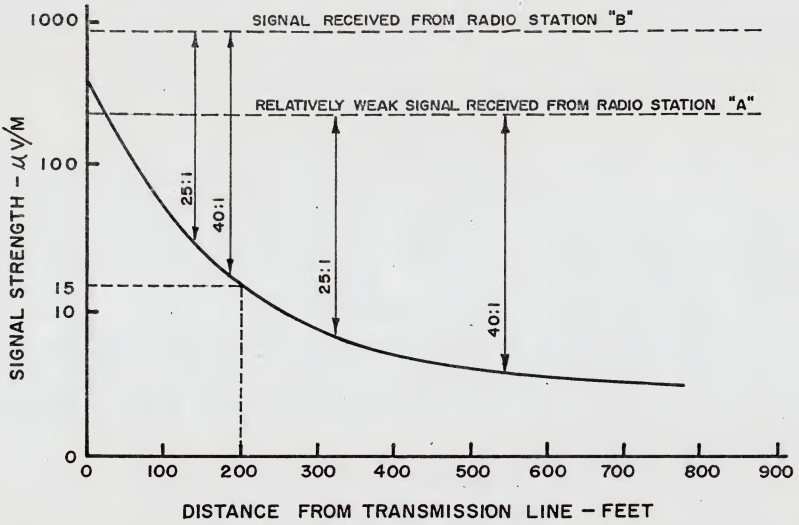

Fig. 8. Radio reception quality adjacent to transmission line.

at a greater distance, say 300 feet, who prefers to listen to station "A" would find the transmission line noise objectionable.

It appears presently unrealistic to establish standard radio noise levels for transmission lines for a number of reasons (IEEE Committee Report 1965):

1. The broadcast station signal strengths and the number of broadcast stations normally receivable differ widely with location. Broadcasting network affiliation may mean a choice of stations carrying the same program.

2. Some lines may be in whole or in part quite remote from population centers while others may traverse high-density regions for their whole length.

3. Topography may be such that the contiguous population centers are shielded from the line (for example, by an escarpment or small ridge).

4. High-density residential areas expect better quality reception than rural areas, but are normally in areas of higher signal strength. The acceptable signal-to-noise ratio thus tending to vary with population density normally is partially compensated.

5. When considering the factor of population density, the residential proportion is the most important, the daily temporary commercial and industrial population not being involved.

It is suggested that an acceptable RI level for a line be based primarily upon a distance from the line (which distance may vary along the length of the line) and upon a thorough analysis of all the factors mentioned and of those line parameters affecting

CHAPTER V

FACTORS AFFECTING RADIO INTERFERENCE

The variables found to significantly affect RI generation in fair weather and rain are:

1) voltage
2) relative humidity (RH)
3) relative air density (RAD)
4) wind speed (absolute value of wind velocity)

Effect of Voltage

One of the important variables affecting RI generation and the RI level of transmission lines is the electric field at the surface of the conductor, a field directly proportional to voltage. Figure 9 shows a typical voltage run for a 2-plover, 38.5 foot configuration. Data, taken on voltage rise and fall, plot reasonably close to a straight line. This relation can be expressed as

$$dB = K(V-V_o) + dB_a \quad V \geq V_o \quad dB \text{ above } 1\mu V \tag{14}$$

where K is a constant related to the conductor characteristic; V is the applied voltage in KV; V_o is the threshold voltage in KV at which corona noise rises above ambient level; and dB_a is the ambient level or value at zero test voltage. The constant K, and of course V_o, both depend on the line configuration (Robertson, et. al., 1961). The ambient dB_a will also change from point to point near the line due to reradiation of broadcast signals, etc.

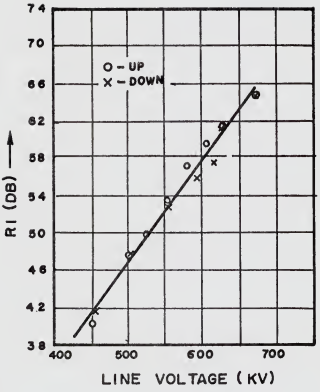

Fig. 9. RI measured 100 feet from outside Phase during fair-weather voltage run. Two Plovers, spaced 38.5 feet.

Effect of RH, RAD, and Wind Speed on Fair Weather RI

In addition to voltage, the relative humidity, relative air density, and wind speed all affect RI level. Since line noise is primarily caused by corona generation at discontinuities on the surface of the conductors, these weather variables affect the generation from points already in corona and the number of points which are in corona. Both season and aging affect the number of surface discontinuities and their character as well; hence, it is not surprising that the effects of the weather variable on RI change somewhat from time to time.

Figure 10 shows that an increase of 10 percent in RH caused an increase of 0.5 dB in RI (LaForest et. al., 1966). Recently, Japanese investigators (Yamada et. al., 1964) reported that as RH increased up to about 85 percent RI decreased, but a large increase in RI occurred for RH values above 85 percent. LaForest, et. al. (1966) mentioned work by Knudsen (1964) on Swedish test lines, who reported a decrease of 2 to 3 dB in RI when RH increased from 45 to 95 percent. This shows that further research is needed in this area.

Figure 11 shows that an increase in RAD of 10 percent decreased RI by 4 dB. This is in good agreement with a decrease of 4.6 dB for an increase of 10 percent in RAD reported from the Japanese investigation.

Figure 12 shows the relation between wind speed and RI level. Three reasons are suggested why an increase in wind may increase RI generation. Increase of wind velocity can bring

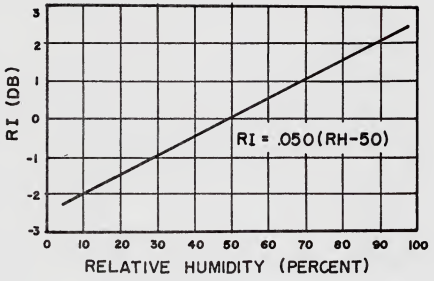

Fig. 10. Effect of relative humidity on fair-weather RI.

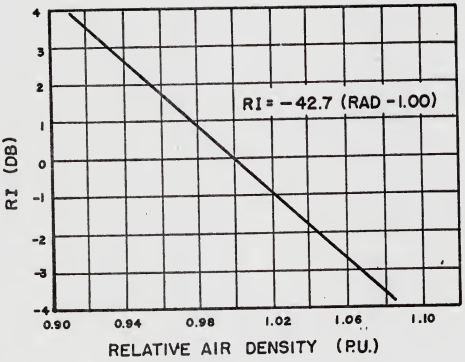

Fig. 11. Effect of relative air density on fair-weather RI.

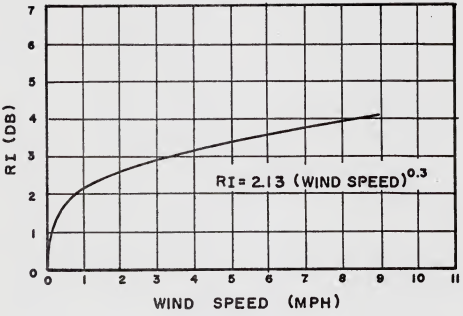

Fig. 12. Effect of wind speed on fair-weather RI.

away from them, and reduce the RAD on the lee sides while increasing it on the windward sides.

Effect of Foul Weather on RI Level

Rain makes some higher voltage lines noiser because of precipitation sparking (Newell, Warburton, 1956). On other lines it has quieting effects because of washing and wetting actions. Rain on pin-type lines evidently short circuits the air gaps existing between tie wires and procelain and line conductors and procelain, and eliminates sparking thereby. It also wets the concrete on suspension strings; rain increases the conductivity between insulator units at connections where rust or oxides or lack of tension in dry weather causes sparking to occur. As with pin-type insulators, it was concluded that suspension-unit concrete absorbs moisture, becomes more conducting and suppresses corona formation.

Dew and fog on most lines are almost as effective as rain. Snow, in many ways, is not much different from rain in influence. On the high voltage lines the distinct pops of the snow flakes on the conductor have been heard in radio receivers. Dry snow scraped and sprinkled on the conductor caused pops. Wet snow will act like water and when blanketing insulators will suppress interference.

Effect of Fault

The noise characteristics on a transmission line during a fault are rather complex, and vary greatly with the particular

condition of the line (Udo and Kawai, 1967). However, from measurements and theoretical analysis it is observed that there is a certain mechanism of noise generation which can satisfactorily explain the actual phenomenon.

When a flashover occurs on a transmission line, a surge voltage generated at the fault point travels along the line to the receiving end, and then oscillates back and forth on the line, reflecting both at the opposite end and the fault point of the line. Each surge induces a noise voltage in a receiving amplifier. The surge is attenuated as it oscillates along the line because of the transmission loss and the generation of earth return components at the fault point in a multi-conductor system. The earth return component of a surge has a large transmission loss compared with the metallic return component.

It was confirmed theoretically as well as experimentally that a high frequency narrow-band noise voltage at the instant of fault almost entirely vanished in 1.5 ms after the occurence of a fault in spite of the high initial value. It can be concluded therefore that there is little danger of noise interference in receiving a signal after some milliseconds pass unless multiple lightening strokes hit the transmission line.

In case of a wide-band noise voltage the noise voltage continues for a longer time than in the case of narrow-band. This means that there is greater danger of noise interference for a wide-band receiver for several milliseconds after an occurence of a fault, except when an extremely large impulse voltage is used as a signal.

In case of a fault through a cracked pin-type insulator, a remarkably large noise voltage was frequently generated due to the particular voltage current characteristic of the insulator. In the case of a fault with a fault current of a few amperes, this high noise voltage lasts for a longer time and makes detection of a radio signal almost impossible. It was found that in the case of a fault current of about 20 amperes, it was generally possible to detect a noise voltage signal about 0.2 seconds after the fault occurrence. The time period becomes longer as the fault currents become smaller.

In an arc fault in air, it was found that a broadband noise of a few hundred volts was generated instantaneously during each half-cycle of the fault current, in the case of a fault current of a few amperes. It was also found that a noise voltage amounted to a few tens of volts in the case of a fault of a few tens of amperes. There is no appreciable noise caused by the arc, if the fault current is more than 200 amperes.

The noise voltage for a flashover of a tree or a suspension insulator string was not much different from that of an arc in the air gap with the same gap length.

Effect of Standing Waves

The RI measurements from short, essentially open-circuited test lines are greatly affected by reflections of radio-frequency energy injected into the system by corona discharges. An interference pattern results, causing standing waves. (LaForest et.

al., 1963). The positions of the maxima and minima of this standing wave are a function of the frequency being measured and the propagation velocity. The effect of these standing waves is amenable to calcualtion and to measurements which were put on a longline basis to allow direct comparisons between the measurements for the several conductor configurations tested. Based on the work of Adams (1956a), a model analysis of RI generation, propagation, and attenuation has been used to predict the behavior of long lines from test line results and short-to-long line conversion factors have been established for each line configuration. Work in this area has also been done by Borthold (1961).

The important factors governing the standing wave pattern are: (1) frequency, (2) length of line, (3) conductor arrangement, (4) attenuation, (5) propagation velocity, (6) bundle characteristics, (7) number of circuits, and (8) terminal impedance.

Typical sections of frequency spectra obtained 100 feet away from the Coldwater line at 500 and 600 KV are shown in Figure 13. The maximum conductor gradients on the 1.108 inch conductors are in the order of 19.5 and 23.4 KV r.m.s./cm for the respective tests. It is also seen from Figure 13 that the difference in noise levels for resonant and nonresonant frequencies at Coldwater is in the order of 20-25 dB, rather than about 30 dB, as for the Ohio Edison's test (Bond et. al., 1963).

Finally from a simple statistical model of the currents and voltages induced in a transmission line by individual corona discharges, it is possible to deduce theoretically these spectral

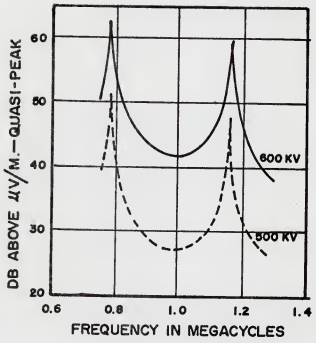

Fig. 13. Typical frequency spectra of Coldwater line at mid-point 100 feet from outer phase (2500 feet long).

densities of the voltages and currents excited in the line. (Helstrom, 1961). By comparing the results for a short line, with their many oscillations as a function of frequency, and for a long line, a method of curve fitting can be developed to allow the prediction of the long-line spectral densities from measurements made on a short test line. When measurements are taken at the center of the line, the geometric mean of the nearest maximum and minimum of the spectral density provides an estimate of the long line value at any frequency. From those estimates it is possible to evaluate the radio noise to be expected from a preactical transmission line of the same design as the test line.

When measurements are not made at the center of the line, the determination of the long-line density is not so direct but Helstrom (1961) has suggested an experimental curve fitting method of doing this.

CHAPTER VI

RADIO INTERFERENCE MEASUREMENT

Radio noise is variable with an extremely wide variation. Therefore, to evaluate the representative performance of a given line at a given voltage (gradient) within a given environment, a sufficient sampling of data is required (IEEE Committee Report, 1965). Present research on transmission line radio noise, therefore, has incorporated small scale data logging facilities. This method of data accumulation is relatively new to the transmission engineer, but data storage may be of such form that modern high-speed high-capacity digital computers can be used to evaluate them. Simultaneous measurement of parameters affecting the levels can be used to establish correlation factors as well as for determining a statistical noise level average.

When streamer corona forms at a point on the conductor two pulse fields exists. A localized or direct field is formed near the streamer, and an indirect field is developed along the line as a result of the pulses traveling down the line. For design of high-voltage lines only the indirect field is considered and the most significant measurements are made with the meter at some distance from the streamer location, especially if the streamer is intense.

A method of measuring RI of a high-voltage transmission line, using meters that conform to American Standard Association (ASA) Standards, has been suggested. This method, while not

perfect, meets the state of the art as it is today, but may well be modified in the future.

For a practical means of measuring RI, it is assumed that the line is of good design, well constructed and maintained, and that spot checks indicate the line to be trouble free. At time of measurement, weather condition should be reasonably the same along the line. Under these conditions, RIV generated on the line should be fairly uniform from end to end.

Line terminations, abrupt transpositions, traps and other discontinuities give rise to standing waves at some frequencies. Test locations where standing waves exist should be avoided when measuring RI in order to obtain consistent and reproducible results. This can be done by selection of test locations (this does not apply to short test sections), at some distance along the line from these discontinuities.

A lateral profile, taken after observing the preceding precaution, is the preferred means of obtaining the immediate RI level of a line. The profile should be obtained at three or more locations fairly well spaced along the line. This proposed method of measurement will provide data that can be compared, with some degree of confidence, to other data taken under similar circumstances.

To measure the corona RI, an antenna is set up near the line and connected to a narrowband filter whose pass frequency can be tuned over the range of interest. The output of the filter is amplified and applied to a rectifying and integrating a-c voltmeter, whose reading is plotted as function of the

input frequency. When a vertical dipole antenna is used, the data can, after proper calibration, be expressed in terms of the mean-square electric intensity per cycle at the antenna. If the antenna stands only a fraction of a wavelength from the line, the measurement can be further related to the spectral density $S(x,f) = \overline{E(x;f)}^2$ of the voltage in the line at the nearest point x. If, instead, a loop antenna is placed on the ground with its axis perpendicular to the line, the rectified filter output measures the mean-square magnetic induction per cycle, which in turn is related to the spectral density $S'(x;f) = \overline{I(x;f)}^2$ of the current passing through point x on the line.

When these measurements are made near a short test line, the data plotted as a function of frequency show numerous peaks and valleys. They represent reinforcement or cancellation of the voltage or current waves by reflection from the ends of the line, and they would be absent from the spectral densities observed near a long transmission line.

The following equipment and techniques are recommended by the Radio Noise Subcommittee (IEEE Committee Report, 1965). Meters shall conform to ASA specifications for radio noise and field strength meters. Meters shall be calibrated at the measuring frequency before and after each set of readings at every measuring location by either a portable external calibrator or a built-in calibrator. A vertical rod antenna with an effective height of 1/2 meter, mounted directly on the meter, is proposed for all frequencies between 0.15 and 25.0 Mc/S. If a

loop antenna is used, it should be rotated for maximum reading and the base of the loop should be 14 inches above ground. If either type of antenna is used in some other manner, the method should be described. The meter shall be placed on the ground at each measuring location with the antenna in a vertical position. The meter reader shall maintain a sufficient distance from the antenna such that his presence will in no way influence the meter reading. A lateral profile RI field shall be measured at midspan, in a plane normal to the line, and at ground level. Measurements locations must be free from other transmission lines, towers, trees, fences, etc. and preferably on level ground. A minimum of three locations as equally spaced along the line as possible shall be used in determining the RI level of a line at the time of measurement. The standard reference frequency shall be 1.0 Mc. Measurements should be made as close to this frequency as possible and the actual frequency stated.

A check shall be made for standing waves by one of the following methods. This may be done by proper selection of measuring frequency and/or test location (short test lines are an exception). Measuring locations should be selected at some distance along the line from discontinuities when possible.

1. At a distance of 50 to 100 feet from and parallel to the line, measure RI at approximately 10 equal consecutive increments for a distance of 500 feet centered at midspan. Standing waves are present if the plotted data of RI vs. distance for a single frequency approximates a rectified sine wave with a maximum to minimum RI of 2 to 1 or greater.

2. At a distance of 50 to 100 feet from the line at approximately midspan, scan the frequency spectrum either manually or automatically throughout the broadcast frequency range. Standing waves are present if somewhat uniformly spaced peaks, with peak-to-valley ratios of 2 to 1 or greater, are observed.

Meters, either indicating or graphic type, shall be installed at one or more of the measuring locations to monitor the line RI while measurements are being made along the line. Readings of RI should be corrected for changes in monitor level, or measurements repeated when conditions are constant. Ambient RI free of station carrier influence at measuring locations shall be at least 6 dB below line RI level. Line voltage at the test locations must be determined as accurately as possible, and specified, for the time during which RI was measured. A sufficient number of measurements shall be made in all seasonal weather conditons so that a statistical assessment may be made. If this is not practicable, a number of measurements shall be made at different times in fair weather to obtain an arithmetic average of the fair weather RI value.

Data shall be recorded in decibels above 1 μv/m (dB = 20 log μv) as read on a quasi-peak detector. Include the following line data:

1. Name of line.
2. Conductor gradients, maximum rms KV/cm.
3. Line voltage.
4. Atmospheric conditions: 1) temperature, °C, 2) relative humidity, 3) pressure, 4) fair, rain, snow.

on samples of actual line conductors since accurate control can then be maintained of such variables as temperature, humidity pressure, and wind, all of which vary over wide ranges in the field. The propagation of noise along the line and distribution of the noise field in a lateral plane depends upon the configuration of the line. The reception and measurement of radio frequency noise are influenced not only by the electrical characteristics of the interference field but also by the design of radio receivers.

Radio interference levels during fair-weather were found to be significantly affected by voltage, relative humidity, relative aire density and absolute value of wind velocity. Noise voltages during a fault vary according to the value of fault current, types of fault, and time interval after the occurence of the fault.

The minima of standing waves in the center of a test line are practically independent of the line attenuation, and are directly related to conductor noise current generation. The geometric mean of the nearest maximum and minimum of the spectral density provides an estimate of the long line value at any frequency.

With the rapid expansion of electric systems and generating capacities in this country and abroad, the number of extra-high-voltage transmission lines has increased enormously during the last decade. Radio interference levels have been important parameters in influencing the conductor types. Considering the large amount of published material on field, laboratory, and theoretical work, it is surprising that many facets of the phenomenon are still in controversy and one basic criterion has

not been resolved, namely the method of rating the performance of a given line from the interference standpoint. Clearly, some common standards of measurement and interpretation of results are necessary before comparative evaluations of designs are meaningful.

REFERENCES

Abboushi, A. K., and L. O. Barthold, "Digital Calculation of Radio Noise Levels," Trans. AIEE (Power Apparatus and Systems), Vol. 80, pp. 841-847, December 1961.

Adams, G. E., "The Calculation of Radio-Interference Level of Transmission Lines Caused by Corona Discharges,"AIEE Transactions, Pt. III (Power Apparatus and Systems), Vol. 75, pp. 411-419, June 1956a.

Adams, G. E., "Wave Propagation Along Unbalanced H-V Transmission Lines," AIEE Transaction, Pt. III (Power Apparatus and Systems), Vol. 78, pp. 639-647, Aug. 1956b.

Adams, G. E., "Recent Radio Interference Investigations on High Voltage Transmission Lines," Proc. Amer. Power Conf., Vol. XVIII, p. 432, 1956c.

Adams, G. E., "An Analysis of the Radio-Interference Characteristics of Bundled Conductors," Trans. AIEE (Power Apparatus and Systems), Vol. 75, pp. 1569-1584, February 1957.

Adams, G. E., "Radio-Interference from High Voltage Transmission Lines as Influenced by the Line Design," Trans. AIEE (Power Apparatus and Systems), Vol. 77, pp. 54-63, April 1958.

Adams, G. E., and L. O. Barthold, "The Calculation of Attenuation Constants for Radio Noise Analysis of Overhead Lines," Trans. AIEE (Power Apparatus and Systems), Vol. 79, pp. 975-981, December 1960.

AIEE Working Group on Definitions, "Definition of Terms Related to Corona," Trans. AIEE (Power Apparatus and Systems), Vol. 82, pp. 1044-1050, December 1963.

American Standard Definitions of Electrical Terms., AIEE, 1942.

Anderson, J. G., M. Baretsky, and D. D. MacCarthy, "Corona Loss Characteristics of EHV Transmission Lines Based on Project EHV Research," IEEE Trans. on Power Apparatus and Systems, Vol. PAS-85, pp. 1196-1212, December 1966.

Bond, C. R., W. E. Pakala, R. E. Graham, and J. E. O'Neil, "Experimental Comparisons of Radio Influence Fields from Short and Long Transmission Lines", Trans. AIEE (Power Apparatus and Systems), Vol. 82, pp. 175-185, April 1963.

Carson, J. R., and R. S. Hoyt, "Propagation of Periodic Current Over a System of Parallel Wires," The Bell System Technical Journal, No. 3, Vol. 6, pp. 495-545, July 1927.

Chevallier, A., "Propagation of High Frequency Waves Along an Electrically Long Symmetric Three-Phase Line (in French)," Revue Generale de l-Electricite, Paris, France, pp. 25-32, January 1945.

Electrical Transmission and Distribution Reference Books, Westinghouse Electric Corporation, 4th Ed., 1950.

Gehrig, E. H., A. C. Peterson, C. F. Clark, and R. C. Redmour, "Bonneville Power Administration's 1[illegible] Current Test Project: II-Radio Interference and Corona Loss," IEEE Trans. on Power Apparatus and Systems, Vol. PAS-86, pp. 278-290, March 1967.

Halleck, M. C., "Calculation of Corona-Starting Voltage in Air-Solid Dielectric Systems," Trans. AIEE (Power Apparatus and Systems), Vol. 75, pp. 211-216, April 1956.

Helstrom, Carl W., "The Spectrum of Corona Near a Power Transmission Line," Trans. AIEE (Power Apparatus and Systems), Vol. 80, pp. 831-837, December 1961.

IEEE Committee Report, "Transmission System Radio Interference," IEEE Trans. on Power Apparatus and Systems, Vol. PAS-84, pp. 714-724, August 1965.

Knudsen, N., "Corona Loss and Radio Interference Measurement at High Voltage A-C on Test Lines in Sweden," CIGRE, Tech, Rept. 411, 1964.

LaForest, J. J., C. B. Lindh, and D. D. MacCarthy, "Radio Noise Corona Loss Results from Project EHV," Trans. AIFE (Power Apparatus and Systems), Vol. 82, pp. 735-750, October 1963.

LaForest, J. J., M. Baretsky, J. R., and D. D. MacCarthy, "Radio Noise Levels of EHV Transmission Lines Based on Project EHV Research," IEEE Trans. on Power Apparatus and Systems, Vol. PAS-85, pp. 1213-1228, December 1966.

Liao, R. W., "Radio Influence Voltages Caused by Surface Imperfections on Single and Bundle Conductors," Trans. AIEE (Power Apparatus and Systems), Vol. 78, pp. 1038-1946, December 1959.

Loeb, Leonard B., "Electrical Coronas; Their Basic Physical Mechanism", University of California Press, 1965.

Mather, R. J. and E. H. Gehrig, "Radio Interference Design Factors for EHV Lines," Proc. Amer. Power Conf. Vol. XXIII, p. 758, 1961a.

Mather, R. J. and B. M. Bailey, "Radio Interference from High Voltage Lines, Part 1-Statistical Approach," Trans. AIEE (Power Apparatus and Systems), Vol. 80, pp. 890-896, December 1961b.

Miller, Charles J., Jr., "Mathematical Prediction of Radio and Corona Characteristics of Smooth Bundled Conductors," Trans. AIEE (Power Apparatus and Systems), Vol. 75, pp. 1029-1037, October 1956.

Miller, C. J., "The Calculation of Radio and Corona Characteristics of Transmission Line Conductors," Trans. AIEE (Power Apparatus and Systems), Vol. 76, pp. 461-475, August 1957.

Morris, R. M., B. Rakaskdas, "An Investigation of Corona Loss and Radio Interference from Transmission Line Conductors at High Direct Voltages," IEEE Trans. on Power Apparatus and Systems, Vol. 83, pp. 5-16, January 1964.

Mostafa, Rabie, Unpublished laboratory investigation performed at Assiut University, U.A.R., with other members of the Department of Electrical Engineering, 1964.

Newell, H. H., and F. W. Warburton, "Variation in Radio and Television Interference from Transmission Lines," Trans. AIEE (Power Apparatus and Systems), Vol. 75, pp. 420-429, June 1956.

Nigol, O. and J. G. Cassan, "Corona Loss Research at Ontario Hydro Coldwater Project," Trans. AIEE (Power Apparatus and Systems), Vol. 80, pp. 304-312, June 1961.

Pearsan, Gary A., "The Effect of Negative Corona Upon the Formation of Positive Corona," Trans. AIEE (Power Apparatus and Systems), Vol. 80, pp. 847-850, December 1961.

Peek, F. W., Jr., "The Law of Corona," Trans. AIEE, Vol. 30, 1911.

Peek, F. W., Jr., "The Law of Corona and the Dielectric Strength of Air-II," Trans. AIEE, Vol. 31, Part I, pp. 1051-1092, June 1912.

Perz, M. C., "Method of Evaluating Corona Noise Generation from Measurements on Short Test Lines," IEEE Trans. on Power Apparatus and Systems, Vol. 82, pp. 833-844, December 1963.

Pipes, L. A., "Matrix Theory of Multiconductor Transmission Lines," Philosophical Magazine, London, England, S. 7, Vol. 24, No. 159, pp. 97-113, July 1937.

Rice, S. O., "Steady-state Solution of Transmission Line Equations," The Bell System Technical Journal, No. 2, Vol. 20, pp. 131-178, April 1941.

Robertson, L. M., W. E. Pakala, and E. R. Taylor, "Leadvill High Altitude EHV Test Project, Part III-Radio Influence Investigations," Trans. AIEE (Power Apparatus and Systems), Vol. 80, pp. 732-743, December 1961.

Skilling, H. H., "Electric Transmission Lines," New York, McGraw-Hill Book Co., 1951.

Taylor, E. R., W. E. Pakala, and N. Kalcio, "The Apple Grove 750-KV Project-515-KV Radio Influence nad Corona Loss Investigations," IEEE Trans. on Power Apparatus and Systems, Vol. 84, pp. 561-560, July 1965.

Udo, Tatsuo, and Mikio Kawai, "Fault Generation Impulse Noise Voltage in a Transmission Line," IEEE Trans. on Power Apparatus and Systems, Vol. PAS-84, pp. 678-684, June 1967.

Waddicor, H., "The Principles of Electric Power Transmission," New York, John Wiley and Sons, Inc., 1928.

Woodruff, L. F., "Electric Power Transmission and Distribution, New York, John Wiley and Sons, Inc., 1925.

Yamada, R., S. Fujii, H. Kondo, and K. Okubo, "Experimental Investigation of Corona on the 800-KV Tanashi Test Transmission Line," CIGRE, Tech. Rept. 404, 1964.

Zenneck, J., "On the Propagation of Electromagnetic Plane Waves Along a Conducting Surface and its Application to Wireless Telegraph (in German)," Annalen der Physik, Leipzig, Germany, Vol. 23, pp. 846-866, 1907.

VITA

Rabie A. F. Mostafa

Candidate for the degree of

Master of Science

Report: CORONA AND RADIO INTERFERENCE ON POWER LINES.

Major Field: Engineering

Biographical:

Personal Data: Born near Minia, U.A.R., May 10, 1942, the son of Abdel-Fadeel Mostafa and Lazima H. Elsharif.

Education: Attended preparatory school in Mallawi, Minia; graduated from Mallawi High School in 1958; received the Bachelor of Science degree in Electrical Engineering from Assiut University, in July, 1963; completed requirements for the Master of Science degree in January, 1968.

Professional experience: Employed by the Department of Electrical Engineering of Assiut University since September, 1963, as Instructor.

CORONA AND RADIO INTERFERENCE ON POWER LINES

by

RABIE ABDELFADEEL MOSTAFA

B. S., Assiut University, U.A.R., 1963

AN ABSTRACT OF A MASTER'S REPORT

submitted in partial fulfillment of the

requirements for the degree

MASTER OF SCIENCE

Department of Electrical Engineering

KANSAS STATE UNIVERSITY
Manhattan, Kansas

1968

ABSTRACT

The background and underlying assumptions of modern analyses applied to corona and radio interference are reviewed. A simple model for the mechanism of corona is discussed, and several important terms are then defined. The results of laboratory tests to show the effect of conductor diameter and phase spacing on the flashover and visual critical corona voltage are presented. Fair and foul weather corona loss and radio noise data from the Project Extra-High Voltage line are presented. Insulator loss and dependence of corona loss on load current are discussed. Emperical equations necessary for the calculation of corona loss and radio interference levels in fair weather are given. The factors affecting corona loss and radio interference are discussed, and noise reaching the customer and acceptable signal to noise ratios are indicated. The radio noise measurements from a test line are correlated with long-line performance. Radio interference measurement equipment and techniques are described.